AD-A096 144 OHIO STATE UNIV COLUMBUS F/G 10/2

PRELIMINARY DESIGN PROCEDURE FOR HIGH POWER DENSITY MHD GENERAT--ETC(U)

DEC 80 P LU

UNCLASSIFIED AFWAL-TR-80-2077 NL

1 OF 1
AD A096 144

END
DATE
FILMED
4-81
DTIC

AFWAL-TR-80-2077

PRELIMINARY DESIGN PROCEDURE FOR HIGH POWER DENSITY MHD GENERATORS

Pau-Chang Lu

Ohio State University
Columbus, Ohio

December 1980

TECHNICAL REPORT AFWAL-TR-80-2077

Final Report for Period June 1978 - August 1978

Approved for public release; distribution unlimited.

AERO PROPULSION LABORATORY
AIR FORCE WRIGHT AERONAUTICAL LABORATORIES
AIR FORCE SYSTEMS COMMAND
WRIGHT-PATTERSON AIR FORCE BASE, OHIO 45433

NOTICE

When Government drawings, specifications, or other data are used for any purpose other than in connection with a definitely related Government procurement operation, the United States Government thereby incurs no responsibility nor any obligation whatsoever; and the fact that the government may have formulated, furnished, or in any way supplied the said drawings, specifications, or other data, is not to be regarded by implication or otherwise as in any manner licensing the holder or any other person or corporation, or conveying any rights or permission to manufacture use, or sell any patented invention that may in any way be related thereto.

This report has been reviewed by the Office of Public Affairs (ASD/PA) and is releasable to the National Technical Information Service (NTIS). At NTIS, it will be available to the general public, including foreign nations.

This technical report has been reviewed and is approved for publication.

James F. Holt

JAMES F. HOLT
Physicist
Energy Conversion Branch
Aerospace Power Division

Joseph Wise

JOSEPH F. WISE
Technical Area Manager
Energy Conversion Branch
Aerospace Power Division

FOR THE COMMANDER

J D Reams

JAMES D. REAMS
Chief, Aerospace Power Division
Aero Propulsion Laboratory

"If your address has changed, if you wish to be removed from our mailing list, or if the addressee is no longer employed by your organization please notify **AFWAL/POOC** *, W-PAFB, OH 45433 to help us maintain a current mailing list".*

Copies of this report should not be returned unless return is required by security considerations, contractual obligations, or notice on a specific document.

AIR FORCE/56780/19 February 1981 — 100

SECURITY CLASSIFICATION OF THIS PAGE (When Data Entered)

REPORT DOCUMENTATION PAGE

READ INSTRUCTIONS BEFORE COMPLETING FORM

19

1. REPORT NUMBER: AFWAL-TR-80-2077

2. GOVT ACCESSION NO.: AD-A096 144

3. RECIPIENT'S CATALOG NUMBER:

4. TITLE (and Subtitle): PRELIMINARY DESIGN PROCEDURE FOR HIGH POWER DENSITY MHD GENERATORS

5. TYPE OF REPORT & PERIOD COVERED: Final Report, June-Aug[redacted]78

6. PERFORMING ORG. REPORT NUMBER:

7. AUTHOR(s): Pau-Chang Lu

8. CONTRACT OR GRANT NUMBER(s): (USAF-ASEE Summer Faculty Research Fellowship)

9. PERFORMING ORGANIZATION NAME AND ADDRESS: Ohio State University, Columbus, Ohio

10. PROGRAM ELEMENT, PROJECT, TASK AREA & WORK UNIT NUMBERS: 37

11. CONTROLLING OFFICE NAME AND ADDRESS: Aero Propulsion Laboratory (AFWAL/POOC), Air Force Wright Aeronautical Laboratories (AFSC), Wright-Patterson Air Force Base, Ohio 45433

12. REPORT DATE: Dec[redacted]80

13. NUMBER OF PAGES: 28

14. MONITORING AGENCY NAME & ADDRESS (if different from Controlling Office):

15. SECURITY CLASS. (of this report): Unclassified

15a. DECLASSIFICATION/DOWNGRADING SCHEDULE:

16. DISTRIBUTION STATEMENT (of this Report)

Approved for Public Release; Distribution Unlimited.

17. DISTRIBUTION STATEMENT (of the abstract entered in Block 20, if different from Report)

18. SUPPLEMENTARY NOTES

19. KEY WORDS (Continue on reverse side if necessary and identify by block number)

MHD Generator, Open Cycle; MHD Generator, High Power Density; MHD Generator, Design; MHD Generator, Scaling; MHD Duct Flow, Isothermal; MHD Generator, Optimization; MHD Generator, Parameter Study.

20. ABSTRACT (Continue on reverse side if necessary and identify by block number)

The steps to be taken in the preliminary design of a high power density, segmented Faraday or diagonal, open-cycle MHD generator are formalized. The recommended design procedure starts with the optimum choice of the combustion chamber pressure. The optimization is based on a semi-empirical expression of the effective power density, developed by Smith and Nichols. As a result of this optimization, a rough estimate of the realizable power density is made, which yields the order of magnitude of the transverse dimension keeping the length-to-diameter ratio around 10 for the desired power output. It is then

DD FORM 1 JAN 73 1473 EDITION OF 1 NOV 65 IS OBSOLETE

SECURITY CLASSIFICATION OF THIS PAGE (When Data Entered)

recommended that the area variation and length be calculated on the basis of an isothermal core flow. This preliminary shape of the duct will serve as the base on which alterations can be made by a computer to accommodate wall effects in the detailed design stage that will follow the preliminary consideration. An alternate route for the preliminary design is provided by using scaling laws. Starting with a well-designed generator which is demonstrably high in power density, dynamically similar units can be produced using these laws. The laws are developed following the modern procedure of ordering. Numerical examples are provided to illustrate the procedure.

FOREWORD

This is the final report on Preliminary Design of High Power Density MHD Generators under the USAF-ASEE Summer Faculty Program (WPAFB), administered by the Ohio State University, from June 5 to 16, and from June 26 to August 18, 1978. The work was conducted at the Aero Propulsion Laboratory of the Wright Aeronautical Laboratories.

Dr. J.F. Holt of the Aero Propulsion Laboratory suggested the present study and the author appreciates the opportunity of the enlightening discussions with him. This report benefited greatly from his editing and constructive criticism.

The author also wishes to recognize Dr. Cecil D. Bailey of Ohio State University, Director of the Summer Faculty Program (1978), for his able and efficient administration which helped make possible the work reported here.

TABLE OF CONTENTS

LIST OF ILLUSTRATIONS

LIST OF TABLES

LIST OF SYMBOLS

A	cross sectional area of (the core of) the generator
a	a constant, see Equation 15
B	magnetic field strength
B^*	peak magnetic field strength
b	proportionality constant of β vs. p
c	a proportionality constant, see Equation 18
c_p	specific heat capacity at constant pressure
E	electric field strength
$F(\ )$	a function
j	electric current density
K	loading factor
L	length of generator
M	Mach number
m	an index
n	an index
p	pressure
p°	combustion chamber pressure
R	gas constant
S	a parameter, page 19
T	temperature (Kelvin)
T°	combustion temperature (Kelvin)
u	flow velocity
W	electric power output

LIST OF SYMBOLS (Concluded)

w	electric power density (per unit volume)
w_{eff}	effective electric power density
x	coordinate in the flow direction
y	a coordinate direction, see Figure 2
α	(Hall field)/(Faraday field)
β	Hall parameter
γ	ratio of specific heat capacities
ρ	density
σ	electric conductivity
$(\ )^*$	reference quantity
$(\ )'$	differentiation with respect to x or (x/L)
$(\tilde{\ })$	dimensionless quantity
$(\ )_i$	at the generator inlet
$(\ )_x$	x-component
$(\ )_y$	y-component
$(\ )_1$	of base design
$(\ )_2$	of scaled (model) design

Units

atm	(standard) atmosphere, a unit of pressure
MW	megawatt
T	tesla (10^4 gauss)

SECTION I

INTRODUCTION

Designing MHD generators for high power density is currently limited to a small circle of practitioners, away from the main stream of commercial MHD activities; the planning is usually done in an ad hoc manner, for individual cases, without stating clearly the approach followed or the philosophy adopted. To render such planning more a science than an art, it is the purpose of this study to formalize the steps to be taken in the preliminary design of a high power density, open cycle segmented Faraday or diagonal combustion-driven MHD generator. The recommended steps are gathered here for one purpose: the realization of maximum possible load power per unit channel volume. Detailed design computations that follow these preliminary steps will undoubtedly indicate trade-off points for a variety of meritorious features.

In obtaining material from a widely scattered literature for the expressed purpose, the author can hardly claim any originality. Although critical comments, personal judgments, minor discoveries, slight extensions and small variations abound, this report is meant to be a designer's guide.

The approach toward achieving high power density will be iterative. Choice of a magnetic field strength profile is regarded as the first among a series of design decisions that will lead to a practical system. The magnetic field strength profile is to be chosen from experience and research of the literature as well as from the following considerations. Use the maximum magnetic flux through the MHD flow consistent with all the usual related pragmatic design factors. These magnet design factors include Hall voltage breakdown limit between MHD channel electrode segments, weight/volume as a function of magnetic field strength, and cost. After going through the preliminary design, the system must be examined to see if the design is practicable. There seems to be no short-cut for arriving at the final practicable design. If the magnetic field profile is not suitably defined in the beginning, the entire process must be repeated with an adjusted profile until the system design is satisfactory. (Although no attempt has been made to computerize the overall design procedure, with much effort one conceivably can build a complex computerized design process that starts with system constraints and arrives at a finely optimized design.)

The design thus starts with a prescribed magnetic field strength profile along the active channel length. In Section II, the recommended design process establishes the combustion chamber pressure, after a brief description of optimization calculations to be done on the inlet Mach number, seeding ratio, and O/F (oxygen to fuel ratio). The optimization is based on a semi-empirical expression of the effective power output developed by Smith and Nichols (Reference 1). This new approach provides a rational basis to the design procedure.

As a result of Section II, estimate of the realizable power density emerges, which will yield the magnitude of the transverse dimension for a fixed length/diameter ratio, for the desired power output.

In Section III, it is recommended that the cross-sectional area variation and the length of the generator be estimated on the basis of an isothermal core flow. The rationale here is as follows: the electrical conductivity of the plasma varies exponentially with temperature; therefore, keeping the entire duct at a uniformly high temperature level would promote high power density. In contrast, a constant velocity design would incur heavy temperature drop and pressure loss; the latter would also burden the diffuser heavily. This preliminary shape of the duct will eventually serve as the base on which variations will be made on a computer to accommodate the boundary effects. The final (computer-aided) design, of course, will not quite come out isothermal.

Section III contains formulas developed for the isothermal core flow through a diagonal conducting-wall generator. To the author's knowledge, these extended formulas for the case of diagonal conducting walls are new.

In Section IV, the preliminary design is carried out along a different route. Starting with any well designed generator which is demonstrably high in power density, either already in operation or in an advanced stage of planning, scaling laws can be applied to produce dynamically similar units for a different power output, and/or a different magnet strength, and/or a different fuel, etc. The procedure can, for example, be used to yield a small dynamically similar pilot unit which can be tested before embarking on a larger-sized endeavor. It must be emphasized here that, if a unit has a power density which is maximum under the given restraints, its dynamically similar models will deliver smaller power per unit volume (being still "high", possibly). However, dynamically similar models will work with equal efficiencies.

The key modeling parameter involved in the scaling laws are established in Section IV following a modern procedure known as the ordering process (see, e.g., Chapter 5 of Reference 2). Modeling (or scaling) is then carried out in the classical manner (see, e.g., Chapter 4 of Reference 3). Although the resulting laws are identical with those quoted in the literature (e.g., Chapter 7 of Reference 4), the derivation presented in this report may be more convincing.

Finally, in Section V, minor losses near the walls are discussed. The discussion is brief since these losses will also be accounted for in the final design--the computer-aided simulation and selection.

It is hoped that designers will find the recommended procedure helpful in providing initial inputs to the design of the magnet, which usually has to be started simultaneously with that of the generator, as well as being helpful in starting the sophisticated computations.

SECTION II

SELECTION OF PRESSURE LEVEL

A modern and operational definition of design is "optimization under partially uncertain constraints." With this definition in mind, one may state a general design philosophy or approach in the form of five steps. Assuming that the operation is not too sensitive to changes of various parameters in a rather large neighborhood of the optimal condition, (1) Establish a rational guideline for the optimization with respect to each parameter. (2) Optimize the object quantity with respect to the parameters one after the other. (3) Display a number of optimal calculations over a range of uncertain values of the constraining parameters. Select a few parameter sets, exercising designer's judgement. (4) Trade off (i.e., deviate from the optimal) for other desired or required characteristics. (5) Model the few cases which exhibit preferred overall characteristics on a computer, and make a final optimization through judicious iterations. The object quantity to be maximized in the above steps is the load power output per unit channel volume, w. At the outset, the fuel used, the oxydizer, and the seeding material are chosen; but these choices are outside the scope of this report. The seeding ratio, O/F ratio, inlet Mach number M_i, and especially the combustion chamber pressure p° are among parameters to be determined. All products of combustion in this report refer to hydrocarbon fuels.

Effective power density is defined as the delivered load power divided by the active channel volume. As a measure of the effective power density when loaded for maximum power under fixed propellant rate, the following semi-empirical formulas from Smith and Nichols (Reference 1) apply:

Segmented Faraday--

$$w_{eff} \sim \begin{cases} \left(\dfrac{1 + \beta^*}{1 + \beta^{*2}}\right)(^1/_4)\sigma^* u^{*2} B^{*2}, & \beta^* > 1 \\ (^1/_4)\sigma^* u^{*2} B^{*2}, & \beta^* \leq 1 \end{cases}$$

Diagonal Conducting Wall--

$$w_{eff} \sim \begin{cases} \dfrac{(\alpha^*\beta^* - 1)^2}{\beta^*(1 + \alpha^{*2})\,(1 + \beta^{*2})}(1/4)\sigma^* u^{*2} B^{*2}, & \beta^* > 1 \\[2ex] \dfrac{(\alpha^*\beta^* - 1)^2}{(1 + \alpha^{*2})\,(1 + \beta^{*2})}(1/4)\sigma^* u^{*2} B^{*2}, & \beta \leq 1 \end{cases}$$

where the asterisk is used to indicate evaluation of quantities at a certain reference point (the MHD channel inlet, for example), and where

β = Hall parameter

σ = conductivity

u = flow velocity

B = magnetic field strength

α = (Hall field strength)/(Faraday field strength)

In an empirical and approximate manner, the formulas account for the internal current leakage and electrode voltage drops.

For a given fuel mixture, temperature level, and B^*, the w_{eff} vs. β^* curve (remembering that $\sigma^* \alpha \sqrt{\beta^*}$ because of the pressure variation) shows a trend as plotted in Figure 1 (the curve marked diagonal conducting walls being roughly for α=-β, a power-maximizing value). An important point is that the illustrated variation of β^* is to be obtained solely through varying the dimensionless pressure $\overset{*}{p}$. (Thus, at the origin, β^*= o, the pressure $\overset{*}{p}$ is infinite). It is thus observed that w_{eff} is maximum when β^*=1.

A rational guideline for the selection of the pressure level now emerges: choose $\overset{*}{p}$ such that $\overset{*}{\beta}$=1, for the given T^* and B^*; if practical constraints force a deviation, it is slightly better to make β^* > 1

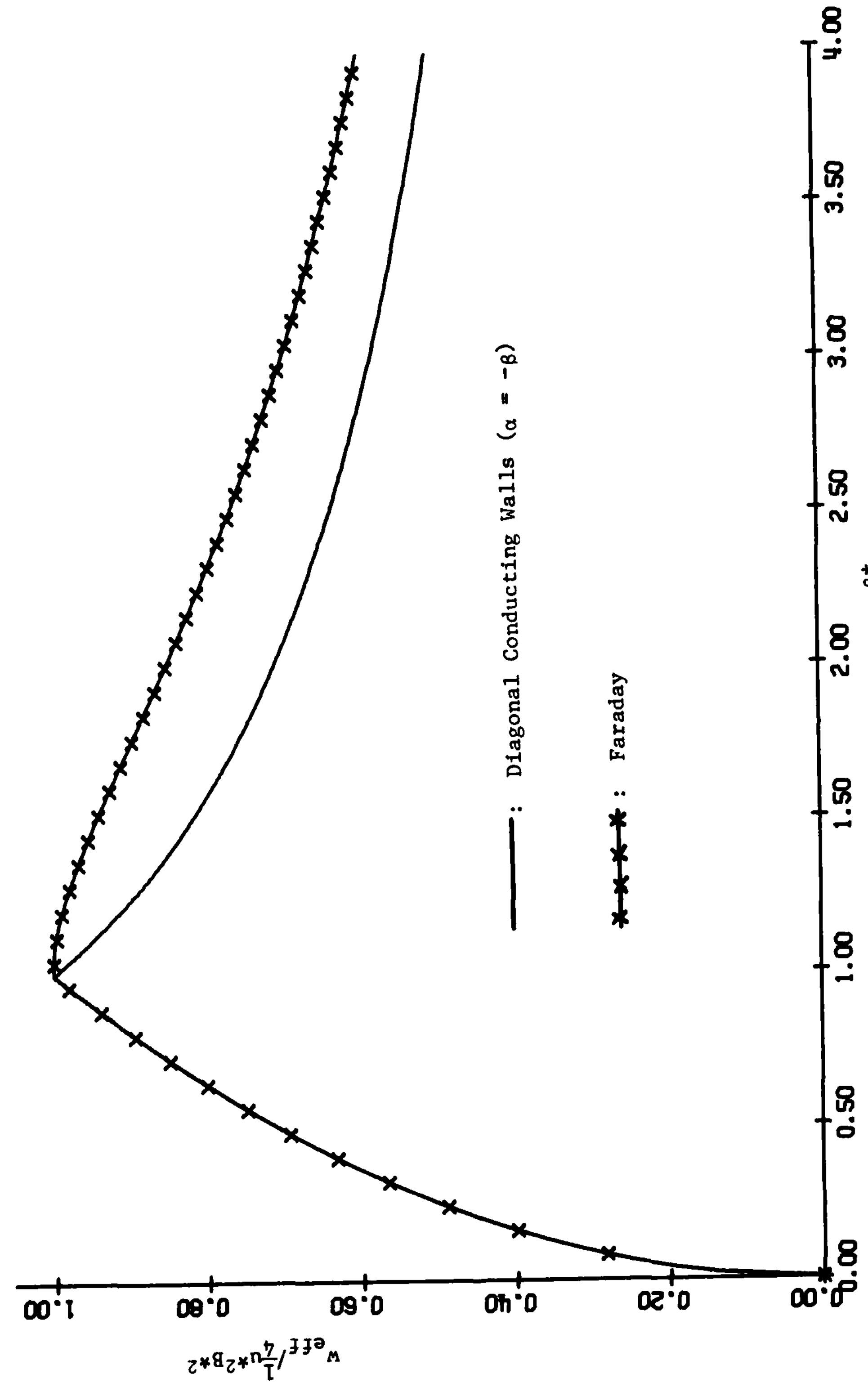

Figure 1. Numerical Relation Between a Measure of w_{eff} and β^*

(rather than <1). The latter preference for $\beta^*>1$ is based on the observation that the limiting Faraday case has a horizontal tangent at $\beta^* = 1$ (on the $\beta^*>1$ side) in Figure 1.

In following this guideline, there is still the question of where to enforce it. Should the asterisk reference point refer to the nozzle exit, or to where the magnetic field peaks, or should one use some kind of average state? Anticipating an isothermal (or, approximately isothermal) design, σ will stay approximately the same everywhere in the core flow. Also, from existing designs where temperature drop is relatively slight, we observe that the flow velocity hardly changes upstream of the peak of the magnetic field. Therefore, it seems desirable to select the pressure value so as to make $\beta=1$ (or somewhat above) at the peak of the magnetic field strength. Thus, with a computer print-out of $\beta(T,p,B)$ in hand, one will select this pressure level accordingly.

Once the pressure at the peak magnetic field strength position is chosen, one can estimate an additional percentage (e.g.,10%) to obtain p_i at the inlet. The combustion pressure can then be calculated for a given entrance Mach number M_i, knowing the ratio γ of the specific heat capacities of the plasma. M_i also links the generator temperature with the combustion gas temperature T°.

As an example, toluene + O_2 + Cs_2CO_3 at the stoichiometric O/F ratio is treated in the manner just described for a peak magnetic field of 4 T. The result is summarized in Table 1. Two effective combustion gas temperatures are employed in the table since the temperature level at the nozzle entrance may be raised somewhat by an increase in combustion pressure, and/or an improvement in the combustion chamber design, etc.

It should be emphasized once again that the optimal pressure level is chosen independently of optimization with respect to the seeding ratio, O/F ratio and inlet Mach number. If all parameters are optimal, the effective power density will be the maximum of maxima; otherwise, it will only be the maximum for a given (non-optimal) set of parameter values. In Table 1, although the Mach number is in the optimal range, the seeding and the O/F ratios are not necessarily optimal.

Alternatively, with the aid of a computer, the effective power density can be optimized with respect to each of the four parameters, seeding ratio, O/F ratio, inlet Mach number, and pressure level. Essentially, the computer is to print out a chart showing the variation of w_{eff} with respect to these parameters; the optimal values are then identified. Less elaborate study (Reference 5) has shown that M_i should always be around 2 for products of combustion to realize maximum power density (which fact is also borne out by a detailed numerical example in (Reference 1). Thus, for a preliminary design, anticipating certain practical ranges of the seeding and O/F ratios (which should be, but might not be, around the optimal value) and M_i (which must be around 2), the pressure level may as well be selected by following the suggested guideline (i.e., to make β=1 where the magnetic field peaks, to estimate p_i by adding a percentage, and to calculate $p°$ based on M_i) as exemplified in Table 1.

Finally, each selection in Table 1 has an anticipated power density associated with it; we will quote four numbers here as illustrations:

10% seeding, M_i = 2.1--

$T° = 3100$ K: $w \sim 60$ MW/m^3

$T° = 3400$ K: $w \sim 320$ MW/m^3

30% seeding, M_i = 2.1--

$T° = 3100$ K: $w \sim 125$ MW/m^3

$T° = 3400$ K: $w \sim 620$ MW/m^3

From these values the generator volume can be estimated for a desired power output. If an empirical length-to-diameter ratio, e.g. 10, is adopted, based on a compromise between end and wall effects, the dimensions of the generator can then be estimated.

TABLE 1

OPTIMAL COMBUSTION-CHAMBER PRESSURE FOR STOICHIOMETRIC COMBUSTION OF TOLUENE AND OXYGEN SEEDED WITH CESIUM CARBONATE (4 TESLA)

	10% Seeding By Weight Of Fuel		30% Seeding By Weight Of Fuel	
M_1	T^o = 3100 K	3400 K	3100 K	3400 K
1.9	p^o = 12 atm	14 atm	7.5 atm	10 atm
2.0	14 atm	16.5 atm	8.5 atm	11 atm
2.1	16 atm	18 atm	10 atm	13 atm
2.2	19 atm	22 atm	12.5 atm	14.5 atm

SECTION III

ISOTHERMAL DESIGN OF A DCW GENERATOR

After selecting the pressure level as discussed in the previous section, the design philosophy calls for determining the isothermal duct shape, i.e., the isothermal core area variation in the flow direction. The result will serve as the base shape upon which the wall effects will be added in the computer simulation that follows the preliminary design. To this end, let us first collect all the governing equations (referring to Figure 2 which describe a general core flow:

$$\rho uA = \text{constant } (= \rho_i u_i A_i) \tag{1}$$

$$\rho uu' = -p' + j_y B \tag{2}$$

$$\rho u\{c_p T' + (u^2/2)'\} = j_x E_x + j_y E_y \tag{3}$$

$$\rho = p/RT \tag{4}$$

$$E_x = \alpha E_y \tag{5}$$

$$K = E_y/uB \tag{6}$$

$$j_x = \{\sigma/(1 + \beta^2)\}(uB)\{\alpha K - \beta(K - 1)\} \tag{7}$$

$$j_y = \{\sigma/(1 + \beta^2)\}(uB)\{\alpha\beta K + (K - 1)\} \tag{8}$$

where prime denotes differentiation with respect to x; subscripts x and y indicate specific components; ρ, A, j, E, R, c_p, and K are respectively the plasma density, cross-sectional area of flow passage, current density, electric field, gas constant of the plasma, specific heat capacity at constant pressure of plasma, and the loading factor; all quantities are local. In Equation 1, ρ_i and u_i are known from the procedure presented in the previous section; A_i can also be decided roughly on the power desired as explained at the end of the previous section.

In the above, Equations 2 through 8 can be easily combined into the following key general equation:

$$(p/RT)c_p T' = p' + \{\sigma/(1 + \beta^2)\}(uB^2)\{\alpha^2 K^2 + (K - 1)^2\} \tag{9}$$

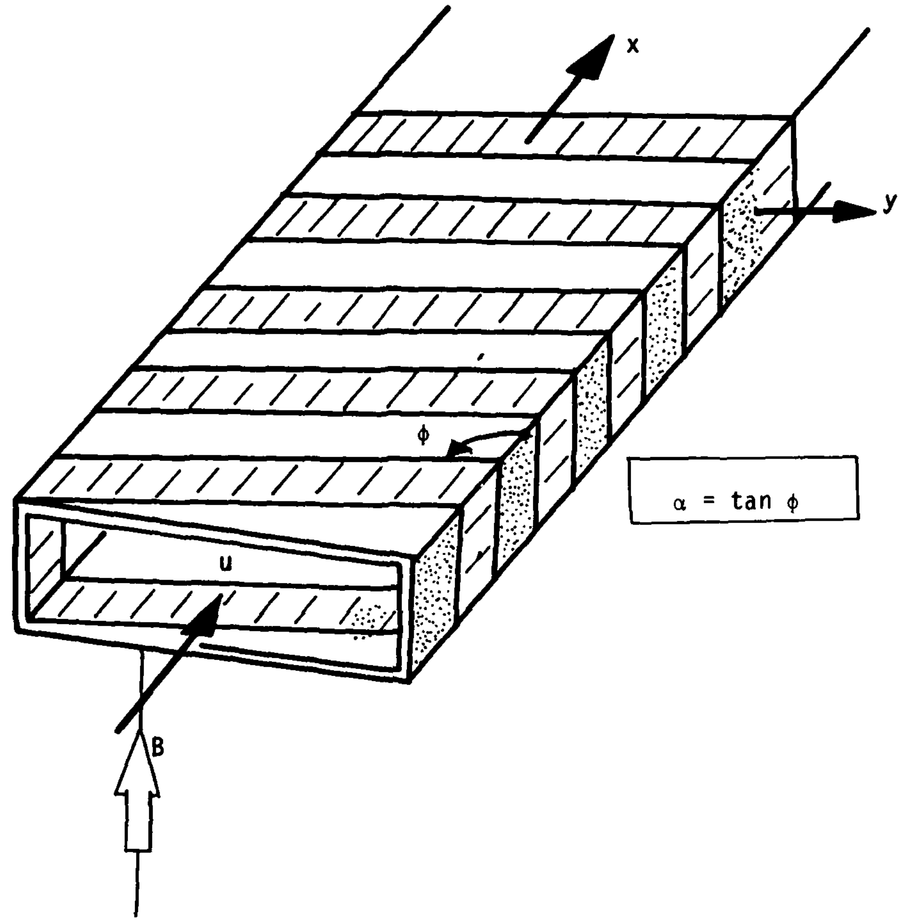

Figure 2. A Duct with Diagonal Conducting Walls

Before we narrow down our scope to the isothermal case, let us point out, in passing, one interesting fact about the general Equation 9: for the case where $\alpha = -\beta$ and $K = 0.5$, it reduces to the form

$$(p/RT)c_pT' = p' + \sigma(uB^2/4) \tag{10}$$

which, being exactly the case for $\beta = 0$ (and $K = 0.5$), has been extensively studied for all values of KO in the literature (see Reference 6 for a unifying approach). The case with $\alpha = -\beta$ and $K = 0.5$ is practically of great interest since $\alpha = -\beta$ maximizes the power density with respect to α, while $K = 0.5$ is not far from being optimal unless β deviates very much from 1. For such a case, all the available solutions in the absence of the Hall effect can be directly employed by substituting 0.5 for K.

Going back now to the isothermal case exclusively, we have from Equation 9

$$p' = -\{\sigma/(1 + \beta^2)\}(uB^2)\{\alpha^2K^2 + (K - 1)^2\} \tag{11}$$

But, from Equation 2 and 8,

$$\{\sigma/(1 + \beta^2)\}(uB^2) = \{\rho\, uu' + p'\}/\{\alpha\beta K + (K - 1)\} \tag{12}$$

Thus, combining Equations 11 and 12, we have

$$p' = -\{\alpha^2K^2 + (K - 1)^2\}\{\rho\, uu' + p'\}/\{\alpha\beta K + (K - 1)\} \tag{13}$$

or

$$K\{K(\alpha^2 + 1) + (\alpha\beta - 1)\}p' = -\{\alpha^2K^2 + (K - 1)^2\}(p/RT)(uu')$$

Integrating, we obtain finally the relation for constant α, β, and K:

$$p/p_1 = \exp\{a(u_1{}^2 - u^2)\} \tag{14}$$

where

$$a = \frac{\alpha^2K^2 + (K - 1)^2}{(2RT)K\{K(\alpha^2 + 1) + (\alpha\beta - 1)\}} \tag{15}$$

For a variable $\beta = b/\rho$, but with $\alpha = -\beta$ and constant K, we have

$$(u_i^2 - u^2)/2RT = \ln\left\{\left(\frac{p}{p_i}\right)^{\frac{K-1}{K}}\left(\frac{p_i^2(K-1)^2 + bK}{p^2(K-1)^2 + bK}\right)^{\frac{2K-1}{2K(1-K)}}\right\} \tag{16}$$

After establishing such a p vs. u relationship, we can go back to Equation 2 and integrate it with respect to x. The result, with the help of Equation 13, is as follows:

$$x = -\int_{p}^{p_i} \frac{(1 + \beta^2)dp}{\{\alpha^2 K^2 + (K - 1)^2\}\ (\sigma u B^2)} \tag{17}$$

where the p vs. u relationship is to be incurred in the integration. Note also that Equation 17 is completely general, with varying σ, β, etc.

In any given case, p(x) obviously will become known at this step; u(x) will then emerge from the p vs. u relationship. Next, since $\rho \propto p$, A(x) can be calculated via Equation 1. To determine the total length of the generator, one sums up the power output along the duct.

Although it is not likely that the exit pressure would turn out lower than 0.2 atm, this value must be checked, since exit pressure lower than 0.2 atm will burden the diffuser heavily. If the magnetic field is high enough that the foregoing procedures yield a pressure level that cause diffuser loading problems, then engineering compromises must be made between diffuser design and magnetic field strength in order to end with a feasible design.

Based on such a preliminary core design, end effects, wall losses, as well as real-gas effects can be added in computer models to yield the adjusted duct shape. It is not known whether the above "almost-isothermal" procedure is actually being used by the designers in the field. But in at least two real cases, both for supersonic and for high power density, the temperature deviation is below 2.5%: it decreases by about 2.3% in the AVCO 400 kW generator (Reference 7), and apparently increases by 1.3% in the Soviet PAMIR I generator (private communication).

SECTION IV

SCALING LAWS

The word "scaling" as used here is restricted to mean dynamic or geometric similitudes among a series of MHD generators. The aim of scaling is to ensure that, once one member of the series is probed extensively, either by actual measurements if it is already operating, or by detailed numerical simulation if it is not yet built, the performance of any other member of the series can be predicted.

The fundamental tool behind scaling is dimensional analysis (or, alternatively, ordering). In principle, every physical phenomenon can be described by a list of dimensionless modeling parameters. Two specific instances of that phenomenon are mutually transformable in a dynamically similar manner if they have the same numerical values for all the dynamic modeling parameters. Scaling, or modeling (see Chapter 4 of Reference 3), calls for keeping the dimensionless parameters the same among individual members of a series.

In practice, if the dimensionless parameters governing a certain phenomenon are many, a dynamically similar series may very well end up containing only one member. The conclusion of the scaling process then becomes degenerate and trivial--namely, every specific instance is only similar to itself. This would be the end of scaling, requiring individual instances be separately probed numerically or experimentally.

In order to have non-trivial scaling, certain dimensionless parameters may have to be allowed to vary from member to member. If the parameters left open in this manner are the geometric ratios and angles, we have a distorted scaling; otherwise, we have a partial scaling.

For MHD generators, the scaling will be severely distorted and will require numerical simulation to compensate for the drastic deviations in scaled design. Since scaling is basically a tool used to provide quick guidelines before detailed analysis, a distorted scaling is of no use to MHD generator design--one might as well skip to numerical simulation directly.

The rest of this section, therefore, is devoted exclusively to the partial scaling of MHD generators.

Applying the ordering process (see Chapter 5 of Reference 2) to Equations 1 through 8 (and thereby ignoring end and wall effects), we introduce the following representative quantities:

Density---- ρ_i

Velocity---- u_i

Area---- A_i

x-coordinate---- Generator length L (which is proportional to $\sqrt{A_i}$ because of geometric similitude)

Magnetic field---- Peak magnetic field B*

Pressure---- p_i

Temperature---- T_i

Conductivity---- σ_i

Current density---- $\sigma_i u_i B^*$

Electrical field----$u_i B^*$

Substituting into these equations the dimensionless quantities $\tilde{\rho} = \rho/\rho_i$, etc., with the tilde signifying nondimensionalization, we have

$$\tilde{\rho}\,\tilde{u}\tilde{A} = 1$$

$$\gamma M_i^{\,2}(\tilde{\rho}\,\tilde{u}\tilde{u}') = -\tilde{p}' + S\tilde{j}_y\tilde{B}$$

$$\tilde{\rho}\,\tilde{u}\{\tilde{T}' + [(\gamma-1)/2]M_i^{\,2}(\tilde{u}^2/2)'\} = [(\gamma - 1)/\gamma]S(\tilde{j}_x\tilde{E}_x+\tilde{j}_y\tilde{E}_y)$$

$$\tilde{\rho} = \tilde{p}/\tilde{T}$$

$$\tilde{E}_x = \alpha\tilde{E}_y$$

$$K = \tilde{E}_y/\tilde{u}\tilde{B}$$

$$\tilde{J}_x = \{\tilde{\sigma}/(1 + \beta^2)\}\ (\tilde{u}\tilde{B})\ \{\alpha K - \beta(K - 1)\}$$

$$\tilde{J}_y = \{\tilde{\sigma}/(1 + \beta^2)\}\ (\tilde{u}\tilde{B})\ \{\alpha\beta K + (K - 1)\}$$

where the prime now denotes differentiation with respect to (x/L). As a result of this process, a number of governing (dimensionless) parameters show up naturally and unambiguously; namely,

$$S = \sigma_i u_i B^{*2} L/p_i$$

$$M_i = u_i/\sqrt{\gamma R T_i}$$

$$\tilde{B} = \tilde{B}(x/L) = \tilde{B}(\tilde{x})$$

$$\tilde{\sigma} = \tilde{\sigma}(\tilde{T}, \tilde{p})$$

$$\beta = \{\tilde{\beta}(\tilde{T}, \tilde{p})\}\ \beta_i$$

$$\alpha,\ K,\ \gamma$$

A series of geometrically similar generators must have the same numerical values or variations (for $\tilde{B}$, $\tilde{\beta}$, and $\tilde{\sigma}$) in order to be dynamically similar, as far as the core is concerned. Out of this list, γ stays around 1.1 for all products of combustion; we can therefore omit it from further consideration.

From the literature, we find that

$$\beta \propto B\sqrt{T}/p$$

and

$$\sigma \propto T^m/p^n$$

where m and n are universal constants depending on the temperature range for all plasmas, but where the proportionality constants differ for different plasmas . That is to say,

$$\tilde{\beta} = \tilde{B}(B^*/B_i)\sqrt{T_i}/p_i$$

and

$$\tilde{\sigma} = \tilde{T}^m/\tilde{p}^n$$

So, $\tilde{\sigma}(\tilde{T}, \tilde{p})$ retains the same form, only the consideration of σ_i is needed. Similarly, although $\tilde{\beta}(\tilde{T}, \tilde{p})$ retains the same form (assuming fixed $\tilde{B}(\tilde{x})$), β_i must be considered.

In practice, α is made close to $-\beta$; so, there is no necessity to include its variation. The loading factor K is either kept constant for a series of generators, or it is to vary only slightly; in addition, its influence on the power density can be estimated using a slug-flow model. Thus, finally the list of governing parameters is reduced to S, M_i, $\tilde{B}(\tilde{x})$, and β_i (with σ_i embedded in S).

These governing parameters are also obtained, for example, by Garrison, Brogan, Nolan, et al. (Reference 8), presumably through standard dimensional analysis. The parameter S also frequently appears in the literature by way of dimensional analysis; but, usually, it is the only one mentioned.

Out of these four remaining quantities, $\tilde{B}(\tilde{x})$ is not likely to be fixed for a series of generators; we will have to start our partial scaling by ignoring the requirement of a fixed $\tilde{B}(\tilde{x})$. The influence of the field strength is then invested only with the peak B* which appears in S and in β_i through B_i . Such a partial scaling has been carried out and applied by Garrison, Brogan, Nolan, et al. (Reference 8). Although it is somewhat fruitful and useful, such scaling yields rather restrictive modeling laws.

Noting that the β-level in a well-designed generator is around 1, and that the influence of the β-level can be assessed separately (e.g., in the manner discussed in Section II), this report will go one step further and recommend a partial scaling based on S and M_i only. By relaxing the requirement that β_i be kept constant from case to case in a series of generators, more productive scaling laws are possible; and the scope of application is suddenly widened. For instance, taking

$$\sigma = cT^{10}/p^{0.5} \tag{18}$$

where c is a coefficient the value of which is available for specific plasmas, we see that S = constant for different cases in a series implies that[1]

$$L \propto p^{1.5}B^{-2}T\text{-}10.5/c \tag{19}$$

where M = constant, i.e.,

$$u \propto T^{0.5} \tag{20}$$

(noting that the molecular masses for all products of combustion stay roughly around 35) is also enforced. Now, the object in building a MHD generator is to realize an electrical power output W which can be calculated by integrating the solutions of Equations 1 through 8 with respect to x. By examining the dimensionless forms of these equations, we conclude that W in the form of a dimensionless parameter must come out a function of (under the present partial scaling) S and M, without the necessity of actually solving the equations. To be more specific, we conclude that

$$W/(\sigma u^2 B^2 L^3) = F(S, M)$$

which yields, since S and M are both kept fixed,

$$W/(\sigma u^2 B^2 L^3) = \text{constant}$$

1 From this point on, the subscript i and superscript * will be omitted for ease of writing.

or

$$W \propto \sigma u^2 B^2 L^3$$
$$\propto cT^{11} B^2 L^3 / p^{0.5} \tag{21}$$

or, in terms of the power density,

$$w \propto cT^{11} B^2 / p^{0.5} \tag{22}$$

Next, combining Equations 19 through 22 in various ways, we have the following additional scaling laws:

$$L \propto W^{0.375} / (c^{0.25} T^{2.75} B^{0.5}) \tag{23}$$

$$p \propto c^{0.5} T^{6.6} W^{0.25} B \tag{24}$$

$$w \propto B^{1.5} c^{0.75} T^{7.7} \tag{25}$$

where Equation 25 is approximate in the sense that $W^{1.125}/L^3$, instead of W/L^3, is regarded as being proportional to w. Furthermore, Equation 23 squared, multiplied by Equation 24, yields

$$W \propto pL^2 / T^{1.1} \tag{26}$$

In applying these scaling laws, one must always bear in mind four things: (1) $\tilde{A}(\tilde{x})$ is fixed; (2) Equations 18 through 20 must be satisfied; (3) there are possible errors in ignoring $\tilde{B}(\tilde{x})$, α, β, and K; and (4) deviations must be anticipated from end and wall losses. To guard against possible misapplications, let us quote here one counter-example: in applying Equation 26 to the same generator, one sees that W is proportional to p; but this is singularly uninteresting, since Equation 19 then dictates that p be fixed (for fixed B, T, and c). A correct interpretation of Equation 26 would be, for example, thus: for a given generator, equipped with a different magnet, the pressure level must be adjusted according to Equation 19 in order to operate in a dynamically similar manner as when the old magnet is used; then (and only then), W will change in direct proportion to p. (If nothing but p is changed, the new operation will not be dynamically similar; and W will not be proportional to p.) We would also like to emphasize that it is the dimensionless quotient $w/\sigma u^2B^2$ that remains fixed from member to member in a series of dynamically similar generators; the power density w definitely will change from case to case. It is especially important to bear in mind that, if a given generator is designed for maximum power density, and if a scaled-down unit is built according to these scaling laws, the smaller unit is going to yield lower power density.

Among the previously quoted scaling laws, Equations 19, 23, 24, and 26 have been derived before by Rosa (Chapter 7 of Reference 4), using an intuitive, heuristic, and simplistic argument (the requirement of fixed M being absent).

In the rest of this section, we will apply some of the scaling laws to scale up or down some existing designs known for their high power densities. We will use subscripts 1 and 2, respectively, to denote the base design and the scaled unit. Temperature and pressure in the combustion chamber are used in the calculations; for fixed Mach number, they are proportional to the temperature and pressure at the generator inlet. The two specific formulas used are Equations 19 and 22 which are rewritten as

$$L_2/L_1 = (c_1/c_2)(p_2/p_1)^{1.5}(B_1/B_2)^2(T_1/T_2)^{10.5} \qquad (27)$$

$$w_2/w_1 = (c_2/c_1)(T_2/T_1)^{11}(p_1/p_2)^{0.5} \qquad (28)$$

The results of the scaling are summarized in Table 2. A detailed description of the base designs is given in the following:

Base Design #1--AFAPL KIVA-1 (Reference 9)

Toluene + O_2, seeded with Cs

$p° = 10$ atm, $T° = 3100$ K

$M_1 = 2$, $B^* = 2.3$ T

$W = 200$ kW, $w = 40$ MW/m^3

$L = 0.7$ m

Inlet dimension 24.9 mm x 99.8 mm

Exit dimension 72.6 mm x 114.3 mm

Base Design #2--Soviet PAMIR-1 (Private communication)

Solid fuel ($c = 2.22 \times 10^{-33}$ (mho/m)(atm)$^{0.5}$(K)$^{-10}$)

$p° = 45$ atm, $T° = 3559$ K

$M_1 = 2.14$, $B^* = 4$ T

$W = 15$ MW, $w = 500$ MW/m^3

$L = 1$ m

Inlet dimension 160 mm x 140 mm

Exit dimension 160 mm x 220 mm

Base Design #3--Maxwell 30 MW Unit (Reference 10)

JP-4 + O_2, seeded with Cs

($c = 8.45 \times 10^{-34}$ (mho/m)(atm)$^{0.5}$ (K)$^{-10}$)

$p° = 30$ atm, $T° = 3530$ K

$M_1 = 2.2$, $B^* = 4$ T

$W = 30$ MW, $w = 200$ MW/m^3

$L = 1.3$ m

Inlet dimension 200 mm x 200 mm

Exit dimension 450 mm x 450 mm

Base Design #4--AVCO VIKING-1 (Reference 11)

Toluene + O_2, seeded with Cs

$p° = 15$ atm, $T° = 3100$ K

$M_1 = 2.2$, $B^* = 2.8$ T

$W = 2$ MW, $w = 47$ MW/m^3

$L = 1.75$ m

Inlet dimension 50 mm x 150 mm

Exit dimension 166 mm x 249 mm

In the calculation, the scaled unit always uses toluene + O_2, seeded with Cs, with $c = 1.68 \times 10^{-33}$ (mho/m)(atm)$^{0.5}$(K)$^{-10}$.

TABLE 2

DESIGN VIA SCALING LAWS

Base Design	Size Factor	T°	4 T	5 T
#1	2x	3100 K	p°= 33.3 atm w = 66.3 MW/m^3 W = 2.8 MW	44.7 atm 89 MW/m^3 3.58 MW
		3300 K	51.4 atm 106 MW/m^3 4.25 MW	69.3 atm 143 MW/m^3 5.7 MW
	1.6x	3300 K	40.1 atm 114 MW/m^3 2.35 MW	
	1.5x	3300 K		57.2 atm 157 MW/m^3 2.6 MW
#2	1x	3100 K	10.5 atm 105 MW/m^3 3.15 MW	14.1 atm 142 MW/m^3 4.25 MW
#3	0.8x	3100 K	10.8 atm 78 MW/m^3 6 MW	14.6 atm 105 MW/m^3 8 MW

TABLE 2

(Concluded)

#4	1x	3100 K	24 atm 75.5 MW/m^3 3.2 MW	32.5 atm 101 MW/m^3 4.3 MW
	0.9x	3100 K	22.5 atm 78 MW/m^3 3.3 MW	30 atm 106 MW/m^3 4.5 MW
#1	1.8x	3100 K	31 atm 68.7 MW/m^3 2 MW	44.7 atm 92.6 MW/m^3 2.7 MW
		3300 K	47.9 atm 110 MW/m^3 3.21 MW	64.6 atm 148 MW/m^3 4.3 MW

SECTION V

LOSSES

The losses near the walls and ends, which are totally ignored in the foregoing sections, will eventually be accommodated in the computer simulation that must intercede between the preliminary design and the actual construction. However, a few qualitative remarks about wall effects are in order.

First of all, since MHD generation is a volume phenomenon, while wall losses are surface phenomena, the percentage loss out of the total power must be proportional to

$$\frac{\text{(Surface of the generator)}}{\text{(Volume of the generator)}} \propto \frac{1}{L}$$

Thus, a larger unit (scaling up) will suffer less from the wall losses, and will have a larger efficiency. (The same trend is to be expected also regarding the end losses, since the end regions will occupy a smaller percentage for larger units.)

Secondly, there is the Reynolds number as a measure of the viscous effect, which is completely ignored in the preliminary design. As a rule of thumb, the scaling should not change the Reynolds number by a factor of more than 3. Obeying this rule, one is usually sure that the viscous effects will change only quantitatively by a rather slight degree (e.g., the friction coefficient is roughly proportional to the one-fifth power of the reciprocal of the Reynolds number; also the disturbance due to wall roughness becomes less for larger units). But, a drastic change in Reynolds number must always be scrutinized carefully, for fear that some qualitative deviation may evolve; the boundary layer may separate from the wall, for instance.

REFERENCES

1. Smith, J. M. and L. D. Nichols, Estimates of Optimal Operating Conditions for Hydrogen-Oxygen Cesium-Seeded Magnetohydrodynamic Power Generator, NASA TN D-8374, 1977.

2. Lu, P.-C., Introduction to the Mechanics of Viscous Fluids, McGraw-Hill Book Co., New York, 1977.

3. Lu, P.-C., Fluid Mechanics: A First Course, Iowa State University Press, Ames, Iowa, 1979.

4. Rosa, R. J., Magnetohydrodynamic Energy Conversion, McGraw-Hill Book Co., New York, 1968.

5. Raeder, J. and G. Zankl, "Influence of the Combustor Parameters on the MHD Generator Performance," Workshop on the Performance of Combustion MHD Generators, Munich, June 26-27, 1972.

6. Bender, E., "One-Dimensional Flow in MHD Generators," AIAA J., Vol. 3, pp. 167-169, 1965.

7. Sonju, O. K., Teno, J., Lothrop, J. W. and S. W. Petty, Experimental Research on a 400 kW High Power Density MHD Generator, AFAPL-TR-71-5, Air Force Aero Propulsion Laboratory, Wright-Patterson Air Force Base, Ohio, May 1971.

8. Garrison, G. W., Brogan, T. R., J. J. Nolan, et al., Development of Design Criteria, Cost Estimates, and Schedules for an MHD High Performance Demonstration Experiment, AEDC-TR-73-115, Arnold Engineering Development Center, Arnold Air Force Station, Tenn., August 1973.

9. Shanklin, R. V., III, Lytle, J. K., Nimmo, R. A., Buechler, L. W. and H. W. Hehn, "KIVA-I Extended Duration MHD Generator Development," AFAPL-TR-75-27, Air Force Aero Propulsion Laboratory, Wright Patterson Air Force Base, Ohio, June 1975.

10. Sonju, O. K. and J. Teno, Study of High Power, High Performance Portable MHD Generator Power Supply Systems, AFAPL-TR-76-87, Air Force Aero Propulsion Laboratory, Wright-Patterson Air Force Base, Ohio, August 1976.

11. Kessler, R., Sonju, O. K., Teno, J., Lontai, L. and D. Meader, MHD Power Generation (Viking Series) with Hydrocarbon Fuels, AFAPL-TR-74, Air Force Aero Propulsion Laboratory, Wright-Patterson Air Force Base, Ohio, November 1974.

☆U.S.Government Printing Office: 1981 — 757-002/391

LMED

8